The University of Sydney

School of Civil Engineering
Sydney NSW 2006
AUSTRALIA

http://www.civil.usyd.edu.au/

Centre for Advanced Structural Engineering

Lateral-Distortional Buckling of Monorails

Research Report No R898

N S Trahair BSc BE MEngSc PhD DEng

June 2009

The University of Sydney

School of Civil Engineering
Centre for Advanced Structural Engineering
http://www.civil.usyd.edu.au/

Lateral-Distortional Buckling of Monorails

Research Report No R898

N S Trahair BSc BE MEngSc PhD DEng

June 2009

Abstract:

This paper is concerned with the elastic lateral-distortional (LD) buckling of single span steel monorail I-beams and its influence on their design strengths. The distortion of a slender web reduces the elastic buckling resistance of an intermediate length beam below its flexural-torsional (FT) resistance.

A finite element computer program was used to study the elastic LD buckling of single span beams. The LD to FT buckling moment ratios were generally higher for simply supported beams with bottom flange central concentrated loads than for uniform bending, and lower for shear centre concentrated loads. For beams with bottom flange loading and unrestrained bottom flanges, there were very significant reductions in these ratios, but they increased when rigid web stiffeners or top flange torsional restraints were provided at the supports. For beams with bottom flange loading and unrestrained bottom flanges, the reductions in the elastic buckling resistance were greater for beams with stocky flanges than for slender flanges.

Approximations were found for estimating the reduced resistances which were generally of high accuracy or conservative, and for estimating the increased resistances caused by elastic and rigid top flange end torsional restraints.

A method of designing steel beams against LD buckling was proposed and its use demonstrated by a worked example.

Keywords: beams, bending, buckling, design, distortion, elasticity, member resistance, monorails, steel, torsion.

Copyright Notice

Lateral-Distortional Buckling of Monorails

N.Trahair@civil.usyd.edu.au

Published by:
School of Civil Engineering
The University of Sydney
Sydney NSW 2006
AUSTRALIA

June 2009

http://www.civil.usyd.edu.au

1. Introduction

Steel I-section beams are often considered to buckle in either local (L) (short wave length) or flexural-torsional (FT) (long wave length) modes (Fig. 1a and b). In the latter case, it is assumed that the member cross-section remains undistorted while buckling laterally and twisting. However, in slender web beams, distortion (Fig. 1c) reduces the long wave buckling resistance, as indicated in Fig. 2. Long wave buckling modes which involve distortion are usually referred to as lateral-distortional buckling (LD).

LD buckling is usually ignored in the design of I-section beams (Fig. 3a) [1, 2, 3, 4] because these usually have webs which are not slender, so that distortion effects are small. An exception is the case of a beam on a seat (Fig. 3b) for which the top flange is unrestrained laterally at the supports.

A similar situation occurs in those monorail beams (Fig. 4) for which the bottom flange is unrestrained laterally at the supports. It has been shown [5] that such monorails have a limited resistance to FT buckling, even when the top flange is unrestrained torsionally, because the bottom flange loading provides a restoring torque to resist buckling. The buckling resistances of monorails are significantly increased by top flange torsional restraints at the supports, but the long wave buckling mode of these monorails may involve significant distortion of the cross-section. The purpose of this paper is to investigate the elastic LD buckling of single span steel monorails.

While there have been many studies of the LD buckling of beams, some of which are summarized in [6], a significant development was made in [7,8], which developed a computer program based on the finite strip method of analyzing the elastic buckling of simply supported thin-walled open section beam-columns in uniform compression and bending [9]. A simple approximate method of analyzing the LD buckling of simply supported I-section members in uniform compression and bending was developed in [6], and extended in [10] to members with more general restraint and loading conditions.

2. Elastic flexural-torsional buckling

2.1. Uniform bending

The elastic FT buckling moment of the simply supported doubly symmetric beam in uniform bending shown in Fig. 5 is given by [11, 12, 13]

$$M_{yz} = \sqrt{\frac{\pi^2 EI_y}{L^2}\left(GJ + \frac{\pi^2 EI_w}{L^2}\right)} \tag{1}$$

in which E (= 200,000 MPa) and G (= 76923 MPa) are the Young's and shear moduli of elasticity, I_y, J and I_w are the minor axis second moment of area, torsion and warping section constants, and L is the length.

2.2. Central concentrated load

The maximum moment M_{FT} = QL/4 at elastic FT buckling of a simply supported doubly symmetric beam with a central concentrated load Q which acts at a distance y_Q below the shear centre axis as shown in Fig. 5 may be closely approximated by using [12]

$$\frac{M_{FT}}{M_{yz}} = \alpha_m \left\{ \sqrt{\left[1 + \left(\frac{0.4\alpha_m y_Q}{M_{yz}/P_y}\right)^2\right]} + \frac{0.4\alpha_m y_Q}{M_{yz}/P_y} \right\} \tag{2}$$

in which

$$P_y = \pi^2 EI_y / L^2 \tag{3}$$

and the moment modification factor α_m which allows for the bending moment distribution is approximated by

$$\alpha_m = 1.35\,. \tag{4}$$

For beams loaded at the bottom flange (y_Q = b_w / 2, in which b_w is the distance between flange centroids), a simpler approximation is given by [5]

$$\frac{M_{FT}L}{\sqrt{EI_y GJ}} = 4 + 4.53K + 0.53K^2 \tag{5}$$

in which

$$K = \sqrt{\frac{\pi^2 EI_w}{GJL^2}} \tag{6}$$

The monorail shown in Fig. 4 has lateral restraints only at the top flange ends, and therefore has no apparent torsional restraint. While it is unlikely that such a monorail would ever be used in practice, it nevertheless has theoretical interest because it is able to resist lateral buckling. This is because the combination of the top flange reactions with the bottom flange load induces restoring torques which resist twist rotation ϕ and prevent lateral deflection u of the load point. The dimensionless elastic FT buckling moments of these monorails may be approximated by using [5]

$$\frac{M_{FT}L}{\sqrt{EI_yGJ}} = 6.5K - 0.13K^2 \tag{7}$$

The solutions of this are significantly lower than those given by Equation 5 for bottom flange loading of beams with full torsional restraints.

3. Elastic lateral-distortional buckling

3.1. Buckling analysis

A finite element method of analyzing the elastic LD buckling of uniform I-section beams under general loading and restraint conditions was developed [10, 14] and tested extensively against the theoretical and experimental findings that were available [7, 12, 15, 16]. The nodal deformations consist of the top (T) and bottom (B) flange lateral displacements u and twist rotations ϕ shown in Fig. 1c and lateral rotations u' ($\equiv \mathrm{d}u/\mathrm{d}z$). This method uses cubic deformation approximations for the variations of u and ϕ with the distance z along each element and a cubic approximation for the web displacements down the web. When there are rigid web stiffeners (RWS) which prevent local web distortion, then some of the deformations are related through

$$\begin{aligned} \phi_T - (u_T - u_B)/b_w &= 0 \\ \phi_B - (u_T - u_B)/b_w &= 0 \end{aligned} \tag{8}$$

This method has been used with 10 elements along the beam length to obtain the results reported in this paper. The beams and loadings considered are shown in Fig. 5 and Table 1, and the end conditions in Table 2 (in which the values of 0 and 1 for RWS indicate the presence or absence of rigid web stiffeners at the supports). The sections of Table 1 were chosen so that the web b_w / t_w did not exceed 75 (design codes [1-4] usually apply severe restrictions to unstiffened webs with higher values) and the flange b_f / $2t_f$ did not exceed 16 (again, design codes usually apply severe restrictions to flanges with higher values).

The results are presented in Fig. 6 by the variations of the ratio M_{LD} / M_{FT} of the elastic LD and FT buckling moments (which provides a correction factor for estimating the effect of distortion on the elastic buckling resistance) with that of the slenderness $\sqrt{(M_L/M_{FT})}$, in which M_L is the elastic local buckling moment. This form of slenderness was chosen because both the LD buckling reductions below M_{FT} and the local buckling moments M_L are significantly affected by the effective web slenderness which is influenced by any restraining effects of the compression flange. Thus $\sqrt{(M_L/M_{FT})}$ can be thought of as a measure of the effective web slenderness. Approximate values of M_L may be obtained as shown in the Appendix.

3.2. Uniform bending

The elastic LD buckling of I-beams in uniform bending has been analysed. The beams are simply supported (lateral deflections and twist rotations of the flanges prevented at the supports - Boundary Condition 1 in Table 2). The beam section is Section C of Table 1, which has the most slender web (b_w / t_w = 75) and the stockiest flange (b_f / $2t_f$ = 4), and the length varies between 1000 mm and 8000 mm. The values of the buckling moment ratio M_{LD} / M_{FT} shown in Fig. 6 generally decrease as the slenderness $\sqrt{(M_L/M_{FT})}$ decreases until local buckling occurs at M_L.

3.3. Central concentrated load at the shear centre

The elastic LD buckling of simply supported (Boundary Condition 1 in Table 2) I-beams (Section C of Table 1) with central concentrated shear centre loading has also been analysed. The values of the buckling moment ratio M_{LD} / M_{FT} shown in Fig. 6 are similar to those for uniform bending at high slenderness $\sqrt{(M_L/M_{FT})}$, but decrease more rapidly as the slenderness decreases.

3.4. Central concentrated load at the bottom flange

The elastic LD buckling of simply supported (Boundary Condition 1 in Table 2) I-beams (Section C of Table 1) with central concentrated bottom flange loading has also been analysed. The values of the buckling moment ratio M_{LD} / M_{FT} shown in Fig. 6 are similar to but greater than those for shear centre loading.

The effects of different boundary conditions on the elastic LD buckling of I-beams with central concentrated bottom flange loading have also been analysed. Allowing twist rotations while preventing lateral deflections of both flanges at the supports (Boundary Condition 2) leads to the significant reductions of the values of the buckling moment ratio M_{LD} / M_{FT} shown in Fig. 6, but allowing lateral deflections and twist rotations of the bottom flange while preventing lateral deflections and twist rotations of the top flange (Boundary Condition 3) leads to somewhat lesser reductions (note that the values of M_{FT} for Boundary Condition 3 are significantly lower than those for Boundary Conditions 1 and 2).

The effects of allowing twist rotations of both flanges while preventing lateral deflections of the top flange at the supports have also been analysed. The reduced elastic FT buckling moments of these beams are approximated by Equation 7. The values of the buckling moment ratios M_{LD} / M_{FT} shown in Fig. 6 are relatively high when there are rigid web stiffeners (RWS = 0) at both supports (Boundary Condition 4), but are significantly reduced when there are no rigid web stiffeners (RWS = 1) (Boundary Condition 5).

4. Single span monorails

4.1. Monorails without torsional end restraints

The effects of distortion on the elastic LD buckling of single span monorails with central concentrated bottom flange loads have been investigated for the case where lateral deflections of the top flanges at the supports are prevented, twist rotations of the top flanges are free, and there are rigid web stiffeners. Nine different cross-sections were considered, with values of b_f / t_f = 128 / 16, 204.8 / 10, and 256 / 8, and b_w / t_w = 200 / 6, 240 / 5, and 300 / 4.

It was found that close approximations M_{LDA} of the elastic LD buckling moments M_{LD} could be obtained iteratively from equations of the type

$$\sqrt{\left(\frac{M_L}{M_{FT}}\right)} = \sqrt{\left(\frac{M_{LDA}}{M_{FT}}\right)} + \frac{k_D (M_{LDA} / M_{FT})^{0.75}}{(1 - M_{LDA} / M_{FT})^{0.75}} \qquad (9)$$

in which M_{FT} is obtained from Equation 7. A family of these equations for different values of the factor k_D are shown in Fig. 7. It can be seen that these provide transitions from the local buckling moments M_L at low slendernesses $\sqrt{(M_L/M_{FT})}$ to the FT buckling moments M_{FT} at high slendernesses.

Approximate values of the factor k for the different cross-sections are shown in Table 3. These indicate that the reductions in the elastic buckling resistance caused by web distortion are greater for beams with stocky flanges (low values of b_f/t_f) than for slender flanges. This is because the resistance of a beam with stocky flanges depends mainly on the flexural stiffness of the compression flange in restraining lateral deflection. This stiffness is proportional to b_f^3/t_f, which is comparatively small for a stocky flange. On the other hand, the resistance of a beam with slender flanges depends more on the combined flexural and torsional stiffnesses of the compression flange in restraining both lateral deflection and twist rotation. This combined stiffness is proportional to b_f^2/t_f^2.

The values of k_D in Table 3 are closely approximated by

$$k_D = \begin{Bmatrix} 1 \\ 0.1b_w/t_w \\ (0.1b_w/t_w)^2 \end{Bmatrix}^T \begin{bmatrix} 0.486 & -0.393 & 0.0746 \\ -0.0678 & 0.0622 & -0.0122 \\ 0.00268 & -0.00165 & 0.000218 \end{bmatrix} \begin{Bmatrix} 1 \\ 0.1b_f/t_f \\ (0.1b_f/t_f)^2 \end{Bmatrix} \quad (10)$$

The accuracy of these approximations is demonstrated in Fig. 8 by the solid points. It can be seen that the ratios of the approximations M_{LDA} to the accurate values M_{LD} are close to 1.00, with most values lying between 0.98 and 1.02, except at low slendernesses $\sqrt{(M_L/M_{FT})}$, where the ratios are lower (and conservative).

4.2. Monorails with rigid torsional end restraints

The effects of distortion on the elastic LD buckling of single span monorails with central concentrated bottom flange loads and rigid torsional end restraints at the top flange have also been investigated. It was found that close approximations M_{LDA} of the elastic LD buckling moments M_{LD} could be obtained by using Equations 9 (with M_{FT} obtained from Equation 5) and 10. The accuracy of these approximations is demonstrated in Fig. 8 by the hollow points.

4.3. Monorails with elastic torsional end restraints

The effects of elastic torsional end restraints on the FT buckling of monorails have been investigated using the computer program PRFELB [12, 15, 16]. It was found that close approximations M_{FT} could be obtained by using the values of M obtained from

$$\frac{(M - M_0)}{(M_\infty - M_0)} = \frac{\alpha_{rz}^*}{(\beta + \alpha_{rz}^*)} \tag{11}$$

in which

$$\alpha_{rz}^* = \frac{\alpha_{rz}}{(\pi GJ / L)(1 + K^2)} \tag{12}$$

$$\beta = 1.15\sqrt{K} \tag{13}$$

M_0 and M_∞ are the FT buckling moments obtained from Equations 7 and 6, respectively, and α_{rz} is the stiffness of each torsional end restraint. The accuracy of this approximation is demonstrated by the hollow points in Fig. 9.

The effects of elastic torsional end restraints on the LD buckling of monorails have also been investigated. It was found that close approximations M_{LD} could be obtained by using the values of M obtained from Equations 11-13 provided the values of M_0 and M_∞ are the appropriate values of M_{LDA} obtained from Equation 9. The accuracy of this approximation is also demonstrated by the solid points in Fig. 9.

5. Design against lateral-distortional buckling

Although design codes generally [1-4] have rules for designing beams against FT buckling which are sometimes used for LD buckling, very few have rules which allow the economical design of monorails which are loaded at or below the bottom flange. The Australian code AS4100 [1] has a general method of design by buckling analysis [17] which allows the direct use of the result of an elastic FT buckling analysis such as those performed for this paper. For this, the elastic buckling moment M_{FT} is used in the equation

$$\frac{M_{bx}}{M_{sx}} = 0.6\alpha_m \left\{ \sqrt{\left[\left(\frac{\alpha_m M_{sx}}{M_{FT}} \right)^2 + 3 \right]} - \left(\frac{\alpha_m M_{sx}}{M_{FT}} \right) \right\} \le 1 \tag{14}$$

to determine the nominal major axis moment resistance M_{bx}, in which M_{sx} is the nominal major axis section resistance (reduced below the full plastic moment M_{px} if necessary to allow for local buckling effects), and α_m is a moment modification factor which allows for the non-uniform distribution of bending moment along the beam. For single span monorails with central concentrated load, α_m = 1.35.

The code rules for design against FT buckling are sometimes used for design against LD buckling. It is consistent with these uses to apply the method of design by buckling analysis to LD buckling by modifying Equation 14 by replacing M_{FT} by the elastic LD buckling moment M_{LD}, so that

$$\frac{M_{bx}}{M_{sx}} = 0.6\alpha_m \left\{ \sqrt{\left[\left(\frac{\alpha_m M_{sx}}{M_{LD}} \right)^2 + 3 \right]} - \left(\frac{\alpha_m M_{sx}}{M_{LD}} \right) \right\} \le 1 \qquad (15)$$

6. Worked example

6.1. Problem

Determine the nominal design moment resistance of a 4.0 m span monorail whose section properties are those of Section A in Table 1 and whose yield stress is f_y = 300 N/mm^2, if the stiffnesses of the end connections and supporting beams are such that the torsional stiffness of each top flange end restraints is α_{rz} = 2E7 Nmm/rad.

6.2. Flexural-torsional buckling

Using Equation 6, K = 0.496
Using Equation 7, M_{FT0} = 141.3 kNm.
Using Equation 5, $M_{FT\infty}$ = 282.2 kNm.
Using Equation 12, α_{rz}* = 0.730
Using Equation 13, β = 0.810
Using Equation 11, M_{FT} = 208.1 kNm.

6.3. Lateral-distortional buckling

Using Equation 18a, k_{f1} = 0.538
Using Equation 18b, k_{f2} = 0.459, so that k_f = 0.459
Using Equation 17, f_L = 5183 N/mm^2
Using Equation 16, M_L = 2330 kNm.
so that $\sqrt{(M_L / M_{FT0})}$ = 4.06 and $\sqrt{(M_L / M_{FT\infty})}$ = 2.87
Using Equation 10, k_D = 0.150
Using Equation 9, M_{LD0} = 138.9 kNm.
Using Equation 9, $M_{LD\infty}$ = 272.9 kNm.
Using Equation 11, M_{LD} = 202.4 kNm.

6.4. Design

Using $M_{sx} = f_y S_x$, M_{sx} = 140.9 kNm.
Using Equation 4, α_m = 1.35
Using Equation 15, M_{bxFT} = 119.2 kNm.
Using Equation 15, M_{bxLD} = 117.6 kNm.

7. Discussion and conclusions

This paper is concerned with the elastic lateral-distortional (LD) buckling of single span steel monorail I-beams and its influence on their design strengths. The distortion of a slender web lowers the elastic buckling resistance of an intermediate length beam below its flexural-torsional (FT) resistance. The LD buckling loads provide a transition from the local (L) buckling loads of short length beams to the FT buckling loads of long length beams.

A finite element computer program was used to study the elastic LD buckling of single span beams. The effects of web distortion were expressed by the variations of the ratios M_{LD} / M_{FT} of the elastic LD to FT buckling moments with the slenderness $\sqrt{(M_L/M_{FT})}$ determined using the elastic local buckling moment M_L. These ratios were generally higher for simply supported beams with bottom flange central concentrated loads than for uniform bending, and lower for shear centre concentrated loads. For beams with bottom flange loading and unrestrained bottom flanges, there were very significant reductions in the ratios M_{LD} / M_{FT}, but these ratios increased when rigid web stiffeners or top flange torsional restraints were provided at the supports.

The effects of beam cross-section were studied for beams with bottom flange loading and unrestrained bottom flanges, and it was found that the reductions in the elastic buckling resistance caused by web distortion were greater for beams with stocky flanges (low values of b_f /t_f) than for slender flanges. Approximations were found for estimating the reduced resistances which were generally of high accuracy, except at low slendernesses $\sqrt{(M_L/M_{FT})}$, when they were generally conservative. Approximations were also found for estimating the increased resistances caused by elastic and rigid top flange end torsional restraints, and for determining the elastic local buckling moments M_L.

It was proposed that steel beams should be designed against LD buckling by adapting the method of design by buckling analysis used or implied in some codes for the design against FT buckling. A worked example was given with a summary of its solution. This example suggests that the reductions in the nominal design strengths of single span I-section monorails of practical proportions with rigid end web stiffeners caused by web distortion are small.

Appendix - Elastic local buckling of I-section beams

The effects of distortion on the flexural-torsional (FT) buckling of I-section beams are greatest for beams with slender webs and stocky flanges, and so investigations of the lateral-distortional (LD) buckling need to consider the possibility of web buckling. Web buckling depends primarily on the web slenderness which also strongly influences LD buckling, but also depends on the flange slenderness. In general there is an interaction between flange and web local buckling.

The elastic local buckling moment M_L of an I-section beam (Fig. 3a) can be expressed as

$$M_L = f_L Z_x \tag{16}$$

in which Z_x is the elastic section modulus and f_L is the maximum stress at elastic buckling. This elastic buckling stress is usually expressed as

$$f_L = \frac{\pi^2 E}{12(1-\nu^2)} \frac{k_f}{(b_f / 2t_f)^2} = \frac{\pi^2 E}{12(1-\nu^2)} \frac{k_w}{(b_w / t_w)^2} \tag{17}$$

in which ν is the Poisson's ratio and k_f and k_w are elastic buckling coefficients.

The variations of k_f with the ratios b_f/b_w and t_w/t_f determined using the program THIN-WALL [9] are shown in Fig. 10. There are two modes of buckling, one when web buckling dominates in which the web is restrained by the flange (low values of k_f), and the other when flange buckling dominates in which the flange is restrained by the web (high values of k_f). The transition between these two modes corresponds approximately to the simultaneous buckling of the flange (at $k_f \approx 0.44$) and web (at $k_w \approx 24.5$). These values are slightly higher than the commonly quoted independent values of 0.425 and 23.9 [11, 13] because the buckle half wavelengths of the flanges and webs are different, while the simultaneous wavelengths in the I-beam are equal.)

The value of the local buckling coefficients can be approximated by using the lesser of the values

$$k_{f1} = \frac{0.4(b_f / b_w)^2}{(0.04 + 0.192 t_f / t_w)^2} \tag{18a}$$

$$k_{f2} = \left\{ 0.41 + 0.22\left(\frac{t_w}{t_f}\right) + 0.19\left(\frac{t_w}{t_f}\right)^2 \right\} - \left\{ 0.024 + 0.002\left(\frac{t_w}{t_f}\right) \right\} \left(\frac{b_w}{b_f}\right)^2 \tag{18b}$$

These approximations are compared with the THIN-WALL values in Fig. 10.

Table 1. Section Properties

Quantity	Units	A	B	C	D	E
b_f	mm	128	128	128	204.8	256
t_f	mm	16	16	16	10	8
b_w	mm	200	240	300	300	300
t_w	mm	6	5	4	4	4
Z_x	mm^3	449.6E3	539.5E3	674.4E3	674.4E3	674.4E3
S_x	mm^3	469.6E3	563.5E3	704.4E3	704.4E3	704.4E3
I_y	mm^4	5.592E6	5.592E6	5.592E6	14.32E6	22.37E6
J	mm^4	0.3639E6	0.3595E6	0.3559E6	0.1429E6	0.09378E6
I_w	mm^6	55.92E9	80.53E9	125.8E9	322.1E9	503.3E9
M_L	kNm	2411	1687	869.6	567.5	256.9

Table 2. End Conditions

(0 ≡ fixed, 1 ≡ free)

Case	u_T	u_T'	u_B	u_B'	ϕ_T	ϕ_B	RWS
1	0	1	0	1	0	0	1
2	0	1	0	1	1	1	1
3	0	1	1	1	0	1	1
4	0	1	1	1	1	1	0
5	0	1	1	1	1	1	1

Table 3. Values of k_D

$0.1b_w / t_w$	$0.1b_f / t_f$		
	0.8	2.048	3.2
7.5	0.11	0.07	0.02
4.8	0.13	0.04	0.015
3.333	0.15	0.025	0.01

References

[1] SA. AS 4100-1998 Steel structures. Sydney: Standards Australia; 1998.

[2] BSI. BS5950 Structural use of steelwork in building. Part 1:2000. Code of practice for design in simple and continuous construction: Hot rolled sections. London: British Standards Institution; 2000.

[3] BSI. Eurocode 3: Design of steel structures: Part 1.1 General rules and rules for buildings, BS EN 1993-1-1. London: British Standards Institution; 2005.

[4] AISC. Specification for structural steel buildings. Chicago: American Institute of Steel Construction; 2005.

[5] Trahair NS. Lateral buckling of monorail beams. Engineering Structures, 2008; 30: 3213-8.

[6] Hancock GJ, Bradford MA, Trahair NS. Web distortion and flexural-torsional buckling. Journal of the Structural Division ASCE 1980; 106 (ST7): 1557-71.

[7] Hancock GJ. Local, distortional, and lateral buckling of I-beams. Journal of the Structural Division ASCE 1978; 104 (ST11): 1787-98.

[8] Hancock GJ. Design of cold-formed steel structures 4th ed. Australian Steel Institute; 2007.

[9] Papangelis JP, Hancock, GJ. THIN-WALL – Cross-section analysis and finite strip buckling analysis of thin-walled structures. Centre for Advanced Structural Engineering University of Sydney; 1997.

[10] Bradford MA, Trahair NS. Distortional buckling of I-beams. Journal of the Structural Division ASCE 1981; 107 (ST2): 355-70.

[11] Timoshenko SP, Gere JM. Theory of elastic stability 2nd ed. New York: McGraw-Hill; 1961.

[12] Trahair NS. Flexural-torsional buckling of structures. London: E & FN Spon; 1993.

[13] Trahair NS, Bradford MA, Nethercot DA, Gardner, L. The behaviour and design of steel structures to EC3 4th ed. London: Taylor and Francis; 2008.

[14] Bradford MA, Trahair NS. Lateral stability of beams on seats. Journal of Structural Engineering., ASCE., 1983; 109 (9): 2212-5.

[15] Papangelis JP, Trahair NS, and Hancock GJ. PRFELB – Finite element flexural-torsional buckling analysis of plane frames. Centre for Advanced Structural Engineering, University of Sydney; 1997.

[16] Papangelis JP, Trahair NS, Hancock GJ. Elastic flexural-torsional buckling of structures by computer. Computers and Structures 1998; 68: 125 - 37.

[17] Trahair NS. Buckling analysis design of steel frames. Journal of Constructional Steel Research, 2009; in press.

Notation

b_f, b_w	flange width and web depth
E	Young's modulus of elasticity
FT	flexural-torsional
f_L	maximum stress at elastic local buckling
f_y	yield stress
G	shear modulus of elasticity
I_y	second moment of area about the y principal axis
I_w	warping section constant
J	torsion section constant
K	$= \sqrt{(\pi^2 EI_w/GJL^2)}$
k_D	distortion factor
k_f, k_w	flange and web local buckling coefficients
L	length
L	local
LD	lateral-distortional
L_e	effective length
M	bending moment
M_{bx}	nominal beam moment resistance
M_{FT}	maximum moment at elastic flexural-torsional buckling
M_L	moment at elastic local buckling
M_{LD}	maximum moment at elastic lateral distortional buckling
M_{LDA}	approximation for M_{LD}
M_{px}	fully plastic moment about the x axis
M_{sx}	section moment resistance
M_{yz}	value of M_{FT} for a simply supported beam in uniform bending
n	number of local buckles
P_y	column elastic buckling load
Q	central concentrated load
RWS	degree of freedom associated with a rigid web stiffener
S_x	effective section modulus
t_f, t_w	flange and web thicknesses
u	lateral deflection
u_B, u_T	lateral deflections of bottom and top flanges
u_B', u_T'	lateral rotations of bottom and top flanges
x, y	principal axes
y_Q	distance of load below shear centre
Z_x	elastic section modulus about x axis
α_m	moment modification factor
α_{rz}	stiffness of flange torsional restraint
α_{rz}^*	see Equation 12
β	$= 1.15\sqrt{K}$
ϕ	twist rotation
ϕ_B, ϕ_T	twist rotations of bottom and top flanges
ν	Poisson's ratio

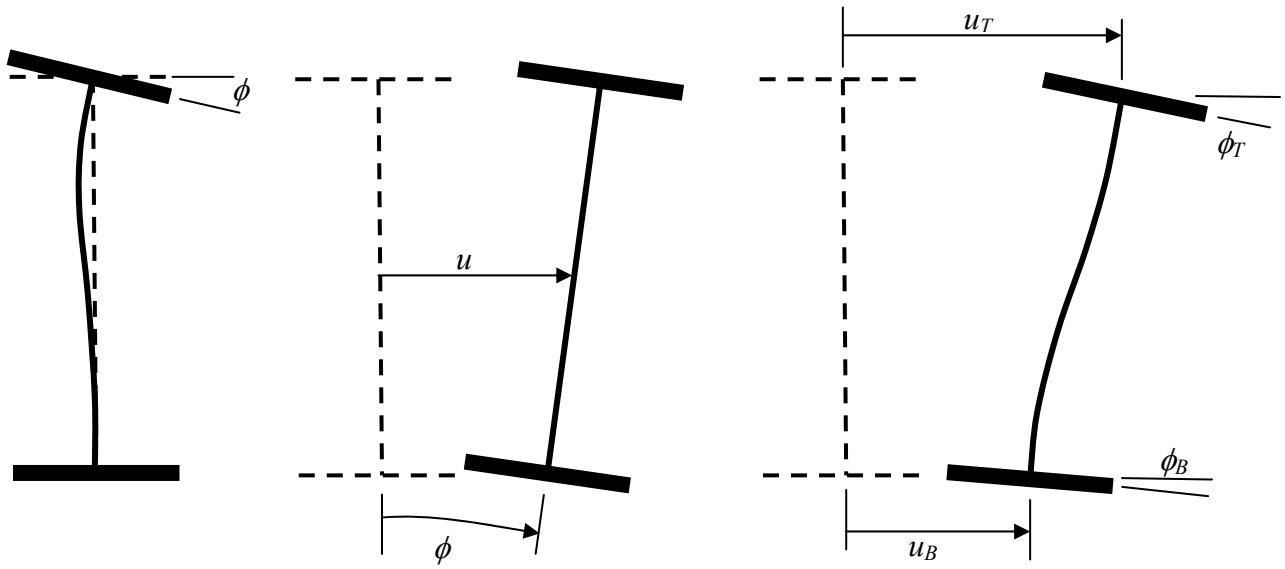

(a) Local buckling (b) Flexural-torsional buckling (c) Lateral-distortional buckling

Fig. 1. Beam Buckling Modes

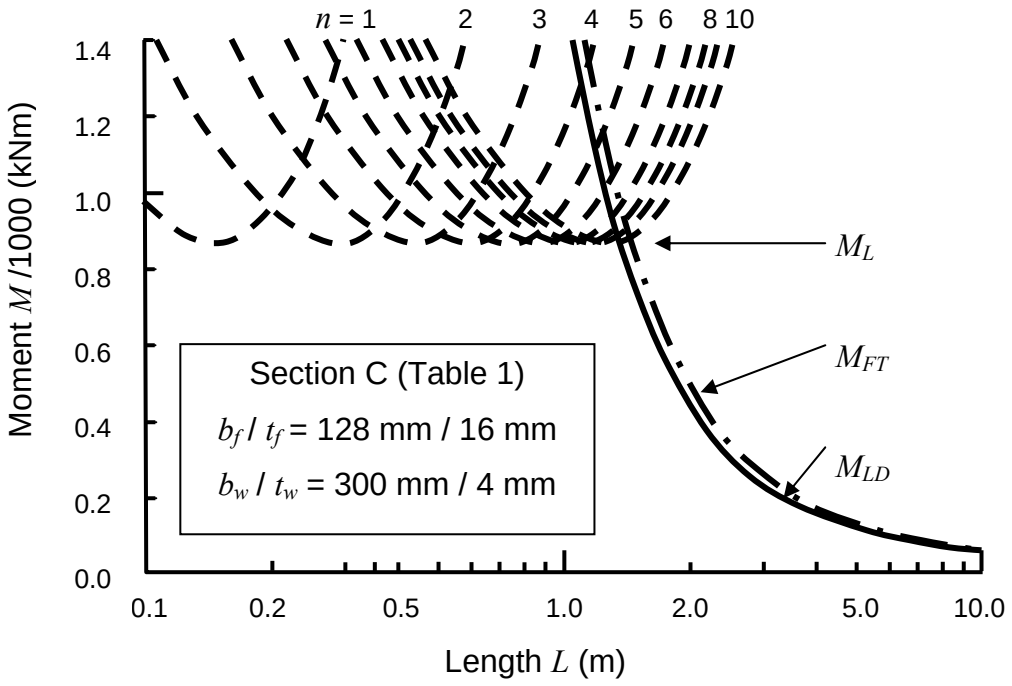

Fig. 2. Effect of Length on Buckling Mode

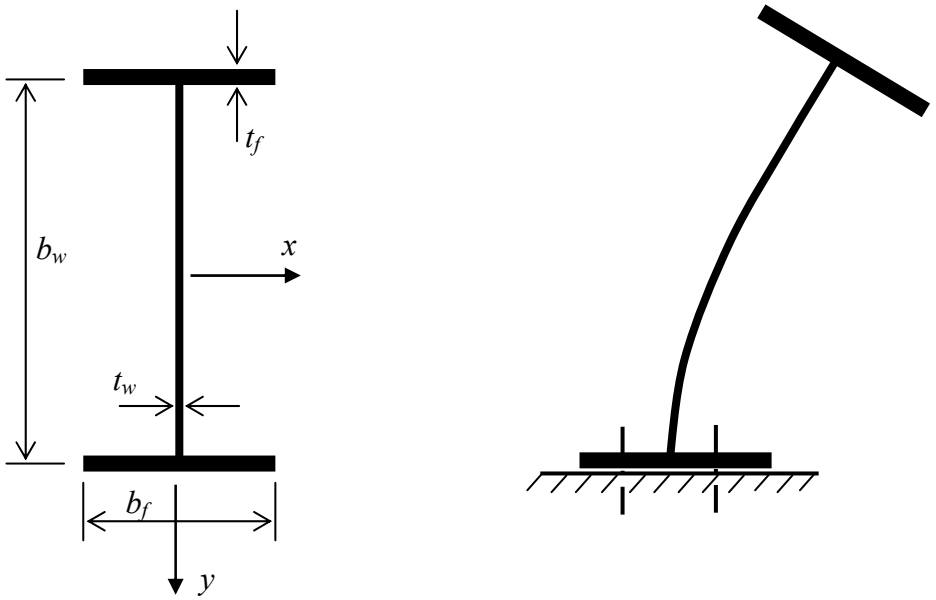

(a) Section

(b) Beam on seat

Fig. 3. Beam on Seat

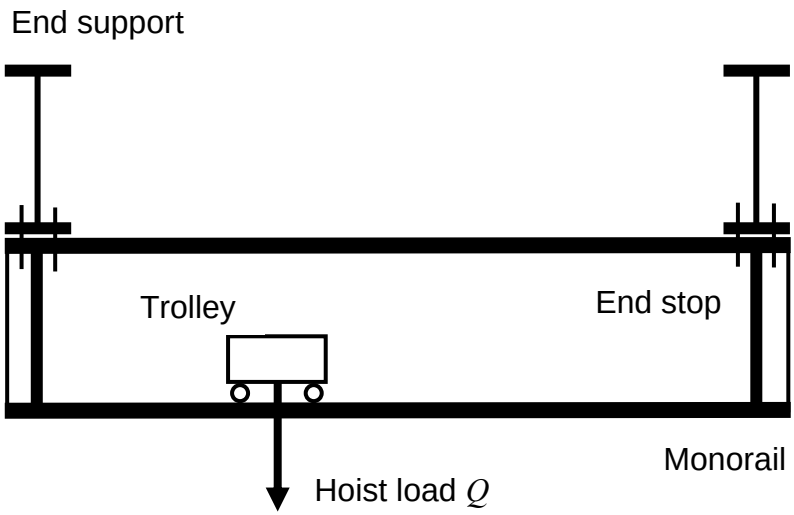

Fig. 4. Single span monorail

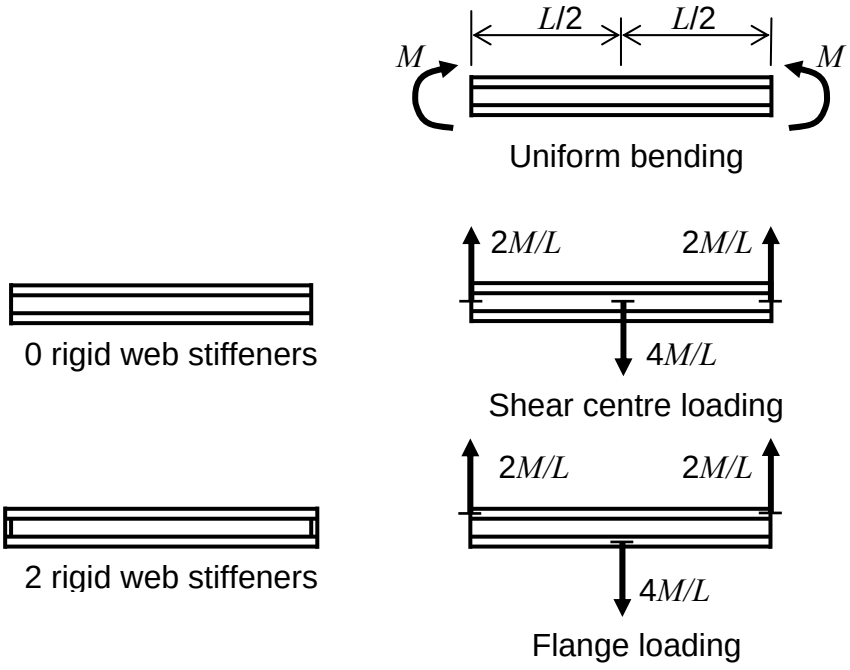

Fig. 5. Beams and Loadings

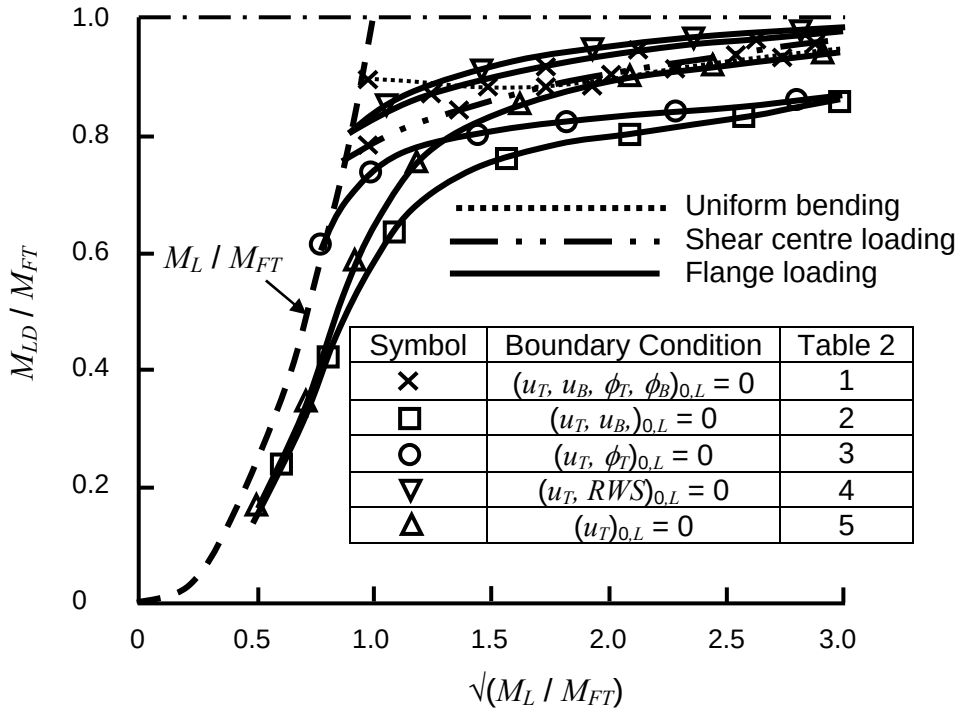

Fig. 6. Effects of Loading and Boundary Conditions

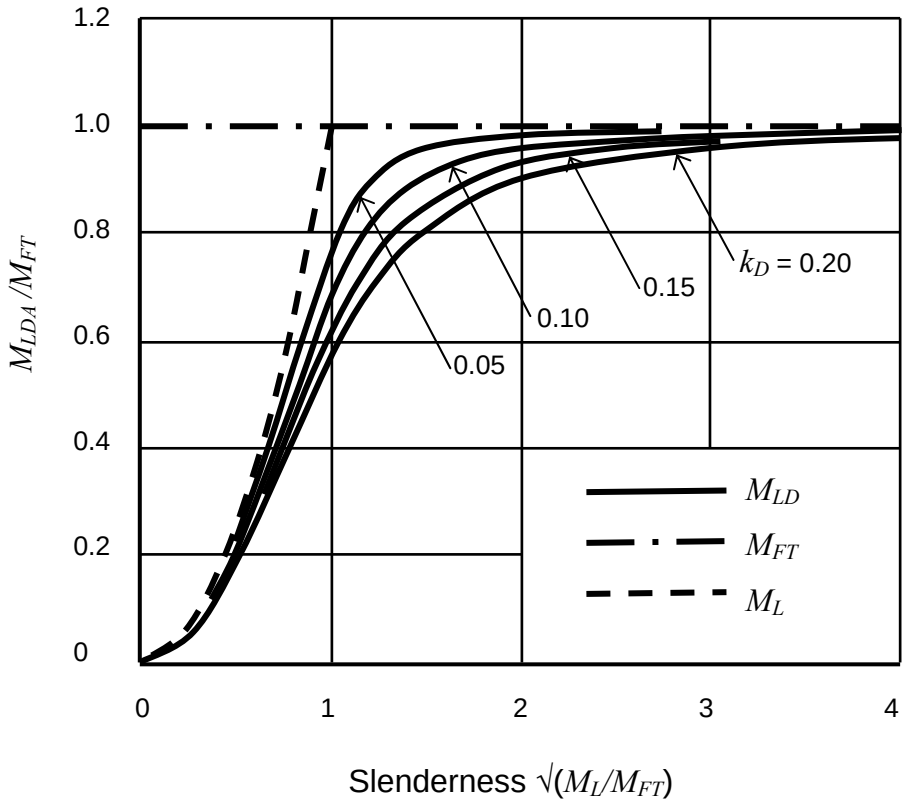

Fig. 7. Family of Approximating Curves

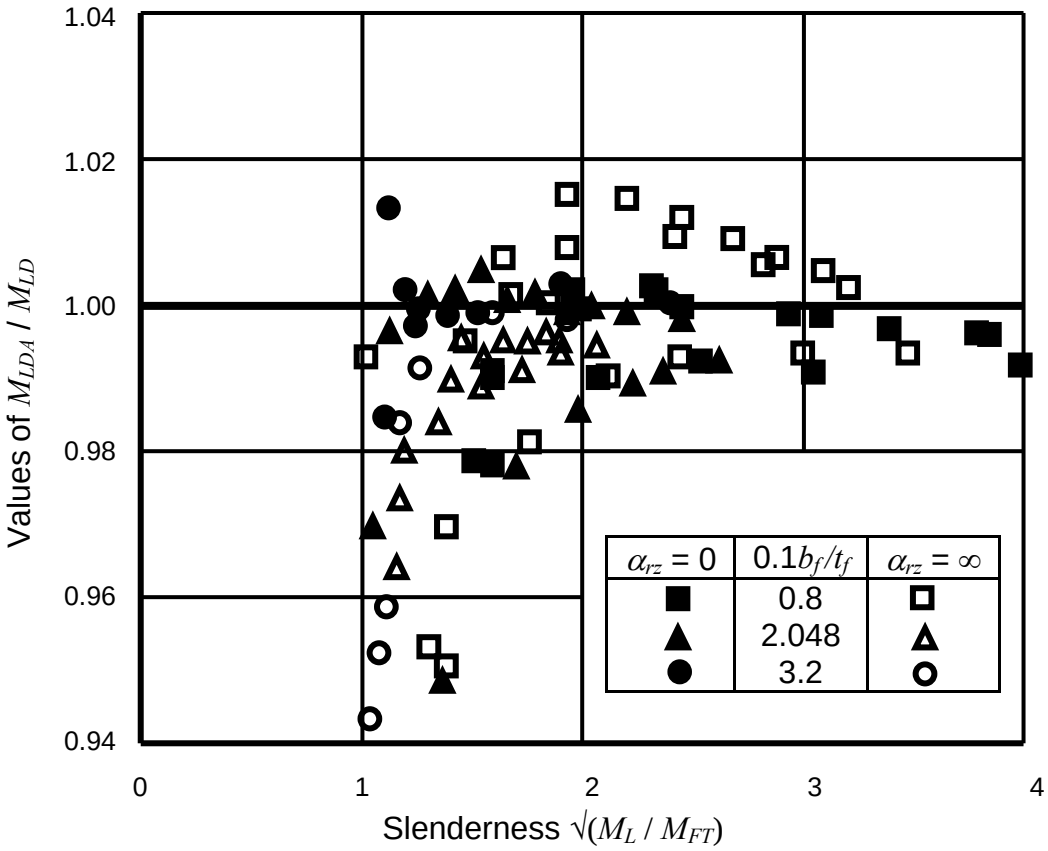

Fig. 8. Accuracy of Approximations

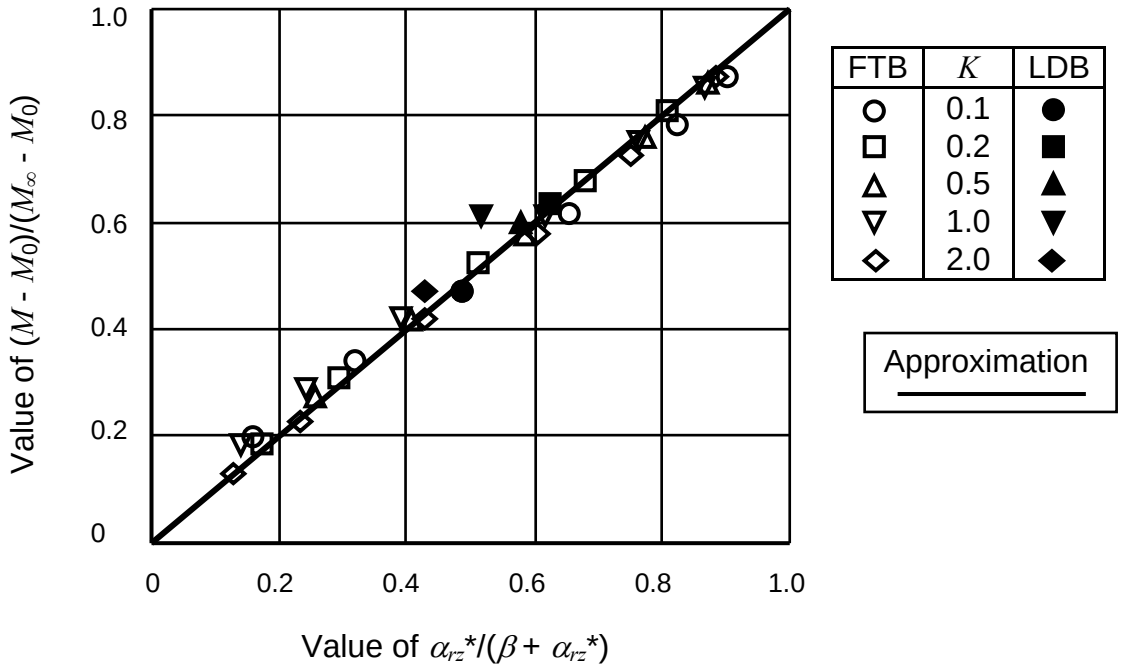

Fig. 9. Elastic Torsional Restraint Approximation

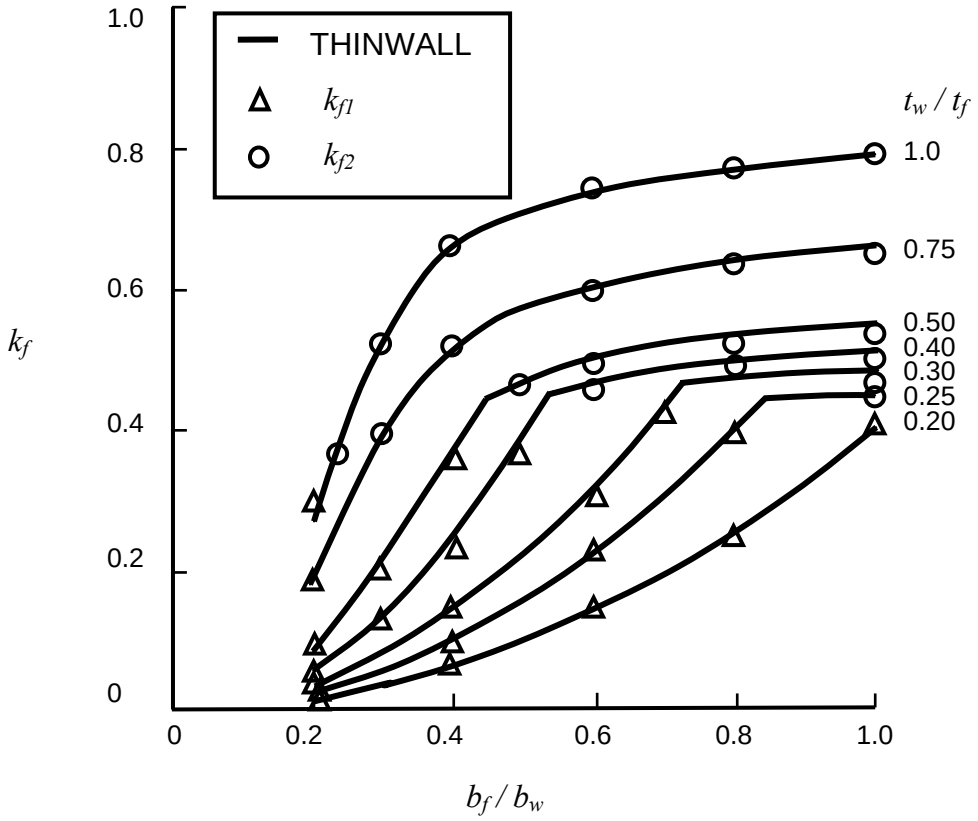

Fig. 10. Local Buckling Coefficients